

## Supplementary Materials for

### **Multidimensional spectroscopy with attosecond extreme ultraviolet and shaped near-infrared pulses**

Hugo J. B. Marroux, Ashley P. Fidler, Daniel M. Neumark\*, Stephen R. Leone\*

\*Corresponding author. Email: srl@berkeley.edu (D.M.N.); dneumark@berkeley.edu (S.R.L.)

Published 28 September 2018, *Sci. Adv.* **4**, eaau3783 (2018)

DOI: 10.1126/sciadv.aau3783

#### **This PDF file includes:**

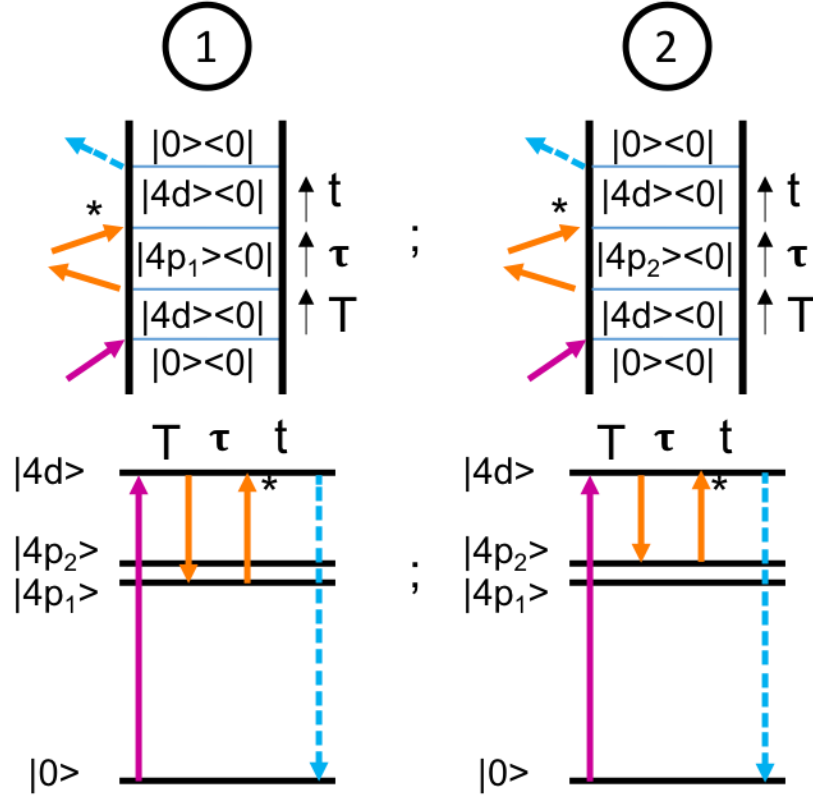
Fig. S1. Double-sided Feynman and Jablonski diagrams of two interfering pathways.

Fig. S2. Pulse characterization.

Fig. S3. Dark-state probing time evolution.

## Supplementary Materials

To demonstrate how equation 1 isolates single state time evolution using pulse shaping, consider two interfering pathways described by the Feynman and Jablonski diagrams in fig. S1.



**Fig. S1. Double-sided Feynman and Jablonski diagrams of two interfering pathways.** The shaped NIR pulses considered in the derivation are indicated by the asterisk.

The derivation of equation 1 is based on the signal field equations obtained from diagrammatic perturbation theory.<sup>25</sup> Signal field equations generated by interaction pathway 1 and 2 in fig. S1 are

$$E_{signal\ 1} \propto e^{(i\omega_{0,4d}-k_{4d})T+i\phi_{XUV}} e^{(i\omega_{0,4p_1}-k_{4p_1})\tau-i\phi_{NIR_1}} e^{(i\omega_{0,4d}-k_{4d})t+i\phi_{NIR_2}}$$

$$E_{signal\ 2} \propto e^{(i\omega_{0,4d}-k_{4d})T+i\phi_{XUV}} e^{(i\omega_{0,4p_2}-k_{4p_2})\tau-i\phi_{NIR_1}} e^{(i\omega_{0,4d}-k_{4d})t+i\phi_{NIR_2}}$$

Where  $\omega_{0,4d}$ ,  $\omega_{0,4p_1}$  and  $\omega_{0,4p_2}$  are the angular frequencies and  $k_{4d}$ ,  $k_{4p_1}$  and  $k_{4p_2}$  the dephasing rates of the  $|4d \rangle \langle 0|$ ,  $|4p_1 \rangle \langle 0|$  and  $|4p_2 \rangle \langle 0|$  coherences, respectively. The phase terms  $\phi_{XUV}$ ,  $\phi_{NIR_1}$ , and  $\phi_{NIR_2}$  are the laser pulse spectral phases at resonant transition energies for the first, second and third interactions, respectively. The transition dipoles and the spatial part of the response function are implicit in the proportionality term. The time delay  $T$  and  $\tau$  are the inter-pulse time delays defined in Fig. 1 while the time delay  $t$  is the emission time delay and is experimentally Fourier transformed by the spectrometer.

To derive the isolated signal using equation 1, the first time delay  $T$  is set to 0 as in the multidimensional experiment probing the dark states in Fig. 3a and 3b. The derivation is also

valid in the case where  $\tau$  and  $T$  are each set to 60 fs, as in the second multidimensional experiment in Fig. 3c and 3d. The two signal fields from interaction pathways 1 and 2 in fig. S1 become

$$\begin{aligned} E_{signal\ 1} &\propto e^{i\phi_{XUV}} e^{(i\omega_{0,4p_1} - k_{4p_1})\tau - i\phi_{NIR_1}} e^{(i\omega_{0,4d} - k_{4d})t + i\phi(\omega_{4d,4p_1})_{NIR_2}} \\ E_{signal\ 2} &\propto e^{i\phi_{XUV}} e^{(i\omega_{0,4p_2} - k_{4p_2})\tau - i\phi_{NIR_1}} e^{(i\omega_{0,4d} - k_{4d})t + i\phi(\omega_{4d,4p_2})_{NIR_2}} \end{aligned}$$

The phase modulation applied is narrow band and will affect the signal field only when it is resonant with the transition energy so the phase dependence of the fields  $E_{signal\ 1}$  and  $E_{signal\ 2}$  on the modulation energy is made explicit.

The signal fields are homodyned by the detector (square law detector) and the recorded signal take the form

$$S(1,0, \omega_{NIR} = \omega_{4d,4p_1}) \propto I_1 + I_2 + 2\Re(E_{signal\ 1} \cdot E_{signal\ 2}^*) \cdot e^{i(\phi(\omega_{4d,4p_1}) - \phi(\omega_{4d,4p_2}))}$$

The intensity terms depend on the  $2k_{4p_1}$  or  $2k_{4p_2}$  decay rates while the interference term decays with a  $(k_{4p_1} + k_{4p_2})$  decay rate and oscillates at the frequency difference  $\omega_{QB} = \omega_{0,4p_2} - \omega_{0,4p_1}$  (Quantum Beats). The pulse shaping aims to isolate each intensity term using narrow band modulations (at  $\omega_{NIR}$ ) to retrieve state specific time information. As described in the main text, the variables in the signal function ( $S$ ) refer to the amplitude and phase modulations at  $\omega_{NIR}$ . When a  $\pi$  phase shift is applied at the resonant frequency  $\omega_{4d,4p_1}$  the signal equation becomes

$$S(1,\pi, \omega_{4d,4p_1}) \propto I_1 + I_2 - 2\Re(E_{signal\ 1} \cdot E_{signal\ 2}^*) \cdot e^{i(\phi(\omega_{4d,4p_1}) - \phi(\omega_{4d,4p_2}))}$$

Where the phase shift is responsible for the minus signs in front of the interference term. By computing the first part of equation 1 the interference term is canceled

$$S(1,0, \omega_{4d,4p_1}) + S(1,\pi, \omega_{4d,4p_1}) \propto 2(I_1 + I_2)$$

The amplitude modulation at  $\omega_{4d,4p_1}$  suppresses terms depending on  $E_{signal\ 1}$  and isolates the intensity term  $I_2$

$$S(0,0, \omega_{4d,4p_1}) \propto I_2$$

By computing equation 1 the intensity term probing the  $4p_1$  state is isolated

$$S(1,0, \omega_{4d,4p_1}) + S(1,\pi, \omega_{4d,4p_1}) - 2S(0,0, \omega_{4d,4p_1}) \propto 2I_1$$

The spectrum, phase, and time profile of the pulse compressed by the pulse shaper are shown in fig. S2a. This pulse corresponds to the step  $S(1,0, \omega_{NIR})$  in the phase cycling scheme. The

pulses used for  $S(0,0, \omega_{NIR})$  and  $S(1, \pi, \omega_{NIR})$  are shown for  $\omega_{NIR} = 700 \text{ nm}$  in fig. S2b and S2c, respectively.

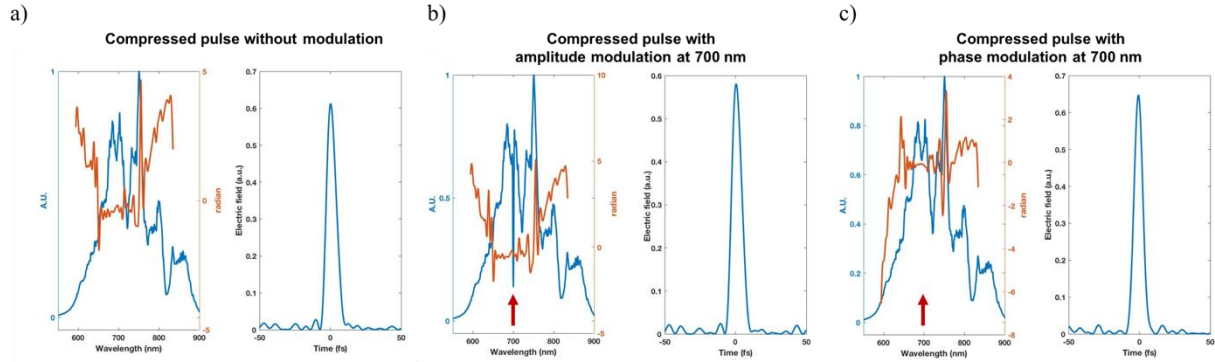


**Fig. S2. Pulse characterization.** a) Compressed pulse. b) Compressed pulse with ten pixels wide amplitude shaping at 700 nm. c) compressed pulse with ten pixels wide phase shaping at 700 nm. The modulated wavelength is indicated by the red arrow.

In agreement with the time trace in Fig. 4b, the time profile is the same for the different pulses. The non-zero amplitude at 700 nm in the amplitude shaped pulse is due to the D-scan spectrometer resolution. The zero amplitude at this wavelength was confirmed using a higher resolution spectrometer. Similarly, the phase shaping does not appear in the pulse's spectral phase in fig. S2c, but appears clearly in the time scan of Fig. 4c.

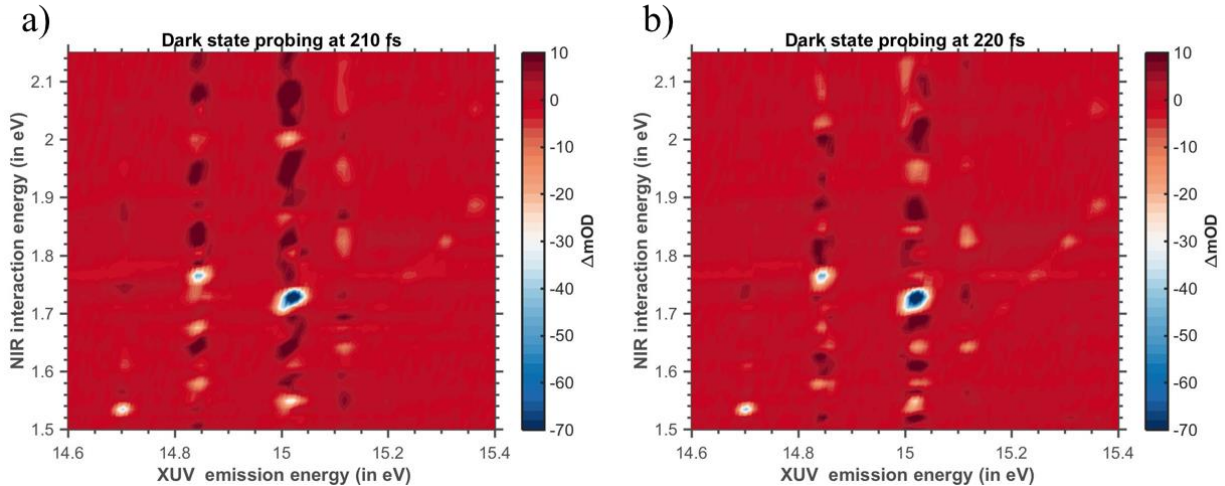


**Fig. S3. Dark-state probing time evolution.** Dark states 2D spectra collected at 210 and 220 fs in a) and b) respectively.

Figure S3 shows 2D spectra probing the dark states evolution at 210 in a) and 220 fs in b). The spectra show similar features for the different time delays confirming the suppression of quantum beat oscillations using the pulse shaping sequence in Equation 1. Small variations between spectra are due to experimental drift.